I-V and Noise Performance in MWIR to VLWIR Large Area $Hg_{1-x}Cd_xTe$ Photodiodes

March 2005

A.I. D'Souza, M.G. Stapelbroek, P.N. Dolan
DRS Sensors & Targeting Systems, 3400 E. Miraloma Avenue, Anaheim, CA 92806

P.S. Wijewarnasuriya*, E.Boehmer
Rockwell Scientific Company, 5212 Verdugo Way, Camarillo, CA 93012

D.S. Smith, J.C. Ehlert, J.E. Andrews
ITT Industries, 1919 W. Cook Rd., Ft. Wayne, IN 46818

* Presently at US Army Research Laboratory, 2800 Powder Mill Road, Adelphi, MD 20783

ABSTRACT

The National Polar-orbiting Operational Environmental Satellite System (NPOESS), is overseen by the Integrated Program Office (IPO), a joint effort of the Department of Defense, Department of Commerce and NASA. Northrop Grumman Space Technology is the prime contractor, responsible for overall system integration as well as the development of the space segment. One of the instruments on the NPOESS satellite is the Cross-track Infrared Sounder (CrIS) instrument. CrIS is a Fourier Transform interferometric infrared (FTIR) sensor used to measure earth radiance at high spectral resolution to derive pressure, temperature, and moisture profiles of the atmosphere from the ground on up. Each CrIS instrument contains three focal plane modules (FPMs), an SWIR FPM [λ_c(98 K) ~ 5.1 μm], MWIR FPM [λ_c(98 K) ~ 9.1 μm] and a LWIR FPM [λ_c(81 K) ~ 15.5 μm]. There are nine large (850 μm diameter) photodiodes per FPM, the nine detectors being arranged in a 3 x 3 array. The nine detectors placement with respect to each other, are under tight tolerances in the X, Y, and Z dimensions. The steps involved in the transfer of photodiodes as part of a newly fabricated wafer to the mounting of the photodiodes on the FPM require a significant amount of dicing, cleaning, wire bonding, baking at elevated temperatures etc.

Quantum efficiency and *1/f* noise in $Hg_{1-x}Cd_xTe$ photodiodes are critical parameters that limit the sensitivity of infrared sounders. The ratio α, defined as the noise current in unit bandwidth i_n(f = 1 Hz, V_d , Δf = 1 Hz) to the dark current $I_d(V_d)$, that is, $\alpha = i_n / I_d$ is one of the parameters used to select photodiodes for placement in FPMs. α is equivalent to $\sqrt{\alpha_H / N}$ that appears in the well-known Hooge expression. For the sixty-one, λ_c ~ 9 μm photodiodes measured at 60 mV reverse bias and at 98 K, the average value of $\alpha = 1.3 \times 10^{-4}$ in the dark and $\alpha_{PHOTO} = i_n / I_{PHOTO}$ is ~ 2×10^{-6} under lluminated conditions. The λ_c ~ 15 μm photodiodes have values of α in the low 10^{-5} range, with the highest performance, diffusion current limited photodiodes having values of α in the mid 10^{-6} range. All the 850 μm diameter, λ_c ~ 15 μm photodiodes measured have excess low frequency noise, with the best performers having i_n(f = 100 Hz, V_d =-60 mV , Δf = 1 Hz) ~ 2×10^{-11} A/$Hz^{1/2}$.

I-V, noise and visual inspections are performed at several steps in the photodiodes manufacturing process. Initial diode *I-V* and visual inspections are conducted at the wafer level. Following wafer dicing, the diodes are placed in leadless chip carriers (LCCs). *I-V*, noise (both in a dark and photo environment), quantum efficiency and visual inspection are performed prior to and following removal of the detectors from Leadless Chip Carriers (LCCs). Finally, the detectors are precision mounted on a FPM base and *I-V*, noise and visual inspections are performed again. It was observed, following FPM fabrication, photodiode dark current and noise had increased from the LCC measurements for some of the nine photodiodes. The performance degradation observed, led to an investigation into the cause (baking at elevated temperatures, mechanical handling, electrical stress *etc.*) of photodiode degradation that occurred between LCC and FPM testing. Correlations between *I-V*, noise and surface visual defects have been performed on some λ_c ~ 15 μm photodiodes. This paper outlines the results of the study, correlating the electrical performance observed to visual defects on the surface and to defects seen following cross sectioning of degraded photodiodes. In addition, other lessons learned and the corrective actions implemented that

led to the successful manufacture of SWIR, MWIR and LWIR large photodiodes from the material growth to insertion into and successful demonstration of flight FPMs for the CrIS program are described.

1.0 INTRODUCTION

Following fabrication of a set of engineering focal plane modules (FPMs) for the CrIS program, photodiode dark currents and noise had increased for some of the photodiodes, as compared to measurements made at the leadless chip carrier (LCC) level. Although degradation in performance was observed for photodiodes from the SWIR, MWIR and LWIR FPMs, the LWIR FPM exhibited the largest number of degraded photodiodes. An example of degraded photodiode performance is shown in figures 1 and 2. Figure 1 shows the I_d - V_d data and the calculated R_d - V_d for the same photodiode measured in an LCC prior to mounting in a FPM and the post mounting measurement of the photodiode in the FPM. The I_d - V_d curve from the LCC measurement was diffusion current limited down to 50 mV reverse bias, whereas the I_d - V_d curve of the same detector mounted in the FPM was limited by a shunt current for reverse bias values greater than ~ 30 mV. The magnitude of the current at V_d = -60 mV (the operating bias) increased by a factor of four and the noise measured at the operating bias, displayed in figure 2, increased by about an order of magnitude. Roll-on at 300 Hz for the module level noise measurement is due to a high-pass filter in the amplifier.

The LWIR module is perceived as the greatest challenge for fabrication because of the very long cutoff wavelength at the relatively high 81 K temperature. In this paper we will specifically discuss results from studies on the LWIR detectors. Roughly similar, but perhaps not quite as severe, effects were observed for the MWIR and SWIR spectral band photodiodes.

The observed performance degradation led to an extensive investigation to determine the cause of the changes occurring between LCC and FPM testing. Potential degradation causes examined were, (i) contamination from adhesives or cleaning solvents used, (ii) ultraviolet light exposure, (iii) inadvertent excess bias applied to the photodiodes, (iv) thermal stress via baking at elevated temperatures, (v) mechanical stress due to photodiode removal or attachment, dicing, wire bonding or (vi) measurement inaccuracy. Results of some of the experiments leading to determination of degradation cause and other lessons learned, such as changes in contact resistance are presented in the. In addition, substantial data on the noise measured in these large photodiodes is presented.

2.0 EXPERIMENT

$Hg_{1-x}Cd_xTe$ layers with x values targeting the bandgap to obtain the appropriate spectral cut-offs were grown by MBE on (211)B CdZnTe (3.5 ±1% Zn) substrates.[1] The 850-μm-diameter active area photovoltaic detectors fabricated in these layers are similar to the 1000-μm-diameter detectors described previously.[2] The detector architecture utilized is a *p*-on-*n* Double Layer Planar Heterostructure (DLPH)[3] in a lateral-collection design[4] that reduces the probability of a performance degrading defect[5,6] intersecting the detector *p*/*n* junction. There are nine 850-μm-diameter photodiodes per FPM,[7] arranged in a 3 x 3 array as shown in figure 1. The placement of detectors with respect to each other is highly precise with tight tolerances in the X, Y, and Z dimensions.

I_d - V_d and noise-versus-frequency measurements[8] are made on all photodiodes that are candidates for inclusion in FPMs. The I_d - V_d measurements are performed utilizing a H-P 4145B semiconductor parameter analyzer. The parameter analyzer is computer controlled via LABVIEW software for data acquisition and analysis. The detector under test is mounted in a temperature-controlled, cryogenic dewar and is electrically connected to an ITHACO 1211 transimpedance current preamplifier for noise measurements.[9]

Separate experiments were conducted to isolate the cause of photodiode degradation. Some of the photodiodes used in the experiments are the previous configuration 1000-μm-diameter[3] detectors. Several potential causes were quickly eliminated. For example, measurement inaccuracy was eliminated by using calibrated equipment, and by duplicating measurements at several locations. In addition, photodiodes that maintained integrity matched photodiode models. No contamination from cleaning solvents or adhesives was observed and exposure to ultraviolet light produced no impact on photodiode performance. The photodiodes are subjected to a 90° C bake for six hours during assembly into the FPM. Also special handling fixtures are used to place the photodiodes in the FPM for precision alignment of the photodiodes with respect to each other. Consequently, the prime

candidates for imparting degradation were narrowed down to baking at elevated temperatures and mechanical stress during wire bond attachment or removal and photodiode die attachment or removal.

3.0 RESULTS AND ANALYSIS

Baking at 90 C

A number of LWIR λ_c(81 K) ~ 15 μm photodiodes were subjected to a cycle of bakes at 90° C and cool downs to 81 K at which *I-V* curves were measured. Figure 3 shows the I-Vs at 81 K of a sample photodiode following cumulative bake times of 2 hours, 8 hours, 16 hours and 32 hours. No change in dark current was observed for reverse bias values greater than 50 mV. The most significant change occurred in forward bias after baking at 90° C for 16 hours. The n-side contact resistance of the photodiode increased from the 100 ohm range to the 800 ohm range following the 16 hour, 90° C bake. This is also evidenced by the change in reverse bias characteristics. Increase in contact resistance has severe deleterious consequences to the quantum efficiency of the photodiode and to the linearity of the CrIS instrument. The contact resistance has been corrected with subsequent photodiodes being manufactured having low contact resistance in the 10 ohm to 20 ohm range. Also, following baking, the contact resistance is maintained at the low pre-bake level. The manufacturing change that corrected the contact resistance issue did not however resolve the cause of degradation in the FPM fabrication cycle.

Baking at 65 °C

Out gassing of the CrIS instrument on the ground and in the NPOESS satellite requires that the instrument and consequently the FPM be subjected to ~ 1000 hour bake at 65 °C. Therefore a FPM labeled Detector Validation Module (DetVal) was assembled using nine λ_c ~ 14.5 μm photodiodes. Noise and I-V measurements were acquired in the dark, at 81 K, as a function of cumulative bake time at 65 °C. The ratio α, defined as the noise current in unit bandwidth i_n(f = 1 Hz, V_d , Δf = 1 Hz) to the dark current $I_d(V_d)$, that is, $\alpha = i_n / I_d$ was in the 1.5 x 10^{-5} to 3.5 x10^{-5} range[9], similar to the values reported earlier for photodiodes with λ_c ~ 15 μm. The α values are plotted in Figure 4 as a function of bake time up to a total cumulative bake time of 1440 hours. The first data point on the X-axis is at 6 hours since the FPM was subjected to a 6 hour 90 °C bake during FPM assembly and prior to the first test. All the photodiodes mounted in this FPM exhibited minimal change in α values except for FOV8 where the α value increased from 2.9 x 10^{-5} to 4.0 x10^{-5}.

Performance Changes from FPM Assembly

Photodiodes are initially mounted in 68 pin LCCs and the I-Vs are measured at 81 K. Wire bonds are then removed and the photodiodes are dismounted from the LCC and cleaned. The photodiodes are then precision mounted on the FPM and wire bonded in order to retest the I-V to check for any changes in photodiode performance due to the handling that occurs between the LCC I-V measurement, and mounting of the photodiode in the FPM. The photodiode shown in figure 5a had no changes in surface visual characteristics and also no changes in reverse bias dark current behavior as seen in figure 5b. The contact resistance decreased marginally, probably due to the four hour 90° C bake the photodiode is subjected to following mounting in the FPM. Similar figures 6a and 6b are shown, the difference in this case being that a scratch was introduced during the wire bonding process that severely degraded the reverse bias characteristics from near diffusion limited behavior into being dominated by a shunt type current.

The primary mechanism for imparting damage to photodiodes that result in performance degradation at the FPM level is the mounting tool for precision pick-up and placement of the photodiodes. Figure 7 is a graph of the *I-V* curves for a λ_c(81 K) ~ 15 μm photodiode before and after damage was imparted during the mounting process to the *p*-side metal covering the 850-μm-diameter lateral collection diode. The *I-V* characteristics changed from being limited by diffusion currents at low reverse bias (out to ~ -50 mV) and tunneling current at higher reverse bias values to almost a short dominated by a shunt-type current. Figure 8 is a picture of the damage sites.

λ_c ~ 9 μm at 98 K Noise Data

Based on wafer level I-V cureves, a number of photodiodes are selected as FPM candidates and measured while mounted in LCCs. Figure 9 is a plot of the noise results for sixty-one, λ_c(98 K) ~ 9 μm photodiodes. Measurements were made at 98K under dark and illuminated conditions. Bias was held at –60 mV. Plotted is the $\alpha = i_n / I_d$ factor defined earlier for each of the photodiodes. Under dark conditions, $\alpha = 1.30 \pm 0.34 \times 10^{-4}$, whereas $\alpha = 2.23 \pm 0.98 \times 10^{-6}$ under illuminated conditions. These values are lower than the $\alpha \sim 2 \times 10^{-4}$ measured in the dark and the $\alpha \sim 4 \times 10^{-6}$ measured previously[9] under illuminated conditions. These lower values are a reflection of the material improvements realized in the past two years since the previous data was acquired.

λ_c ~ 15 μm at 81 K Noise Data

I-V and noise was measured on seventy-three λ_c(81 K) ~ 15 μm photodiodes held at –60 mV at T = 81 K. The noise current i_n at 100 Hz is plotted versus the dark current $I_d(V_d = -60$ mV) in Figure 10a and versus the dynamic impedance $R_d(V_d = -60$ mV) in Figure 10b. As can be seen from both the plots as expected, the lowest noise photodiodes have the lowest dark current and the highest dynamic impedance. Also of note, is the distribution in performance gets wider as the dark current increases and the dynamic impedance decreases. There exists a curve for this set of photodiodes that envelops the best diode performance as a function of dynamic impedance. As the dynamic impedance decreases the best photodiode for that particular dynamic impedance has a lower limit value. This lower limit envelope seems to have an asymptotic behavior, i.e. even as the dynamic impedance keeps increasing, the noise stays constant. Under dark conditions, $\alpha = 1.30 \pm 0.71 \times 10^{-5}$.

Time Series Noise Data

During the course of the investigation to determine the cause of detector degradation, several observations were made. Some of these observations tend to enhance understanding of issues surrounding LWIR HgCdTe photodiode performance, whereas other observations may serve to cloud the issue, depending on ones point of view. As stated earlier, baking of photodiodes at 90 C resulted in understanding the need for adjusting the contact structure to insure stable and low contact resistance. In another case, while measuring the noise in an illuminated LWIR photodiode at 81 K, using a dynamic signal analyzer in the time series mode, the current switched between two discrete states. Each current state was ~ 5 nA on either side of a mean total current of ~ 300 μA. A time series of the current measured with the mean subtracted out is shown in figure 11. Data shown is 0.5 seconds of a total of 2.5 seconds worth of data, the interval between each point is 125 μs. A histogram derived from the data shown in figure 11 is plotted in figure 12. Plotted in figure 13 is the number of occurrences that the photodiode resided in either the high or low state versus the period that it resided in each of the two states. This may be an indication of carriers being trapped and emitted from a defect state. The lifetime is calculated from figure 13 to be 17.69 ms in the high state and 12.08 ms in the low state. This phenomenon corrected itself when subjected to a warm-up to room temperature followed by a cool-down and re-measurement at 81 K, that is the photodiode annealed out the "defect" when warming up to room temperature.

4.0 CONCLUSIONS

The precision positioning of nine large photodiodes during the assembly of a CrIS FPM requires utilization of tools, epoxy that requires curing and customized wire bonding procedures. Following assembly of the first CrIS engineering unit, it was discovered that some of the photodiodes had degraded in electrical performance when compared to pre FPM assembly testing in LCCs. It was initially believed that the 90° C bake in the assembly cycle was causing the degradation. However, baking at 90° C for up to 32 hours showed no increase in reverse bias dark current. Serendipitously, a contact resistance issue was uncovered during the baking experiment, the issue however being promptly corrected in subsequent fabrication cycles. It was finally discovered that excessive wire bonding tip force and/or pressure applied to the surface by the precision positioning tool could damage the surface, the CdTe passivation layer or the HgCdTe layer. A redesigned positioning tool has now corrected any problems related to precision placement of the CrIS photodiodes in the FPM. A separate FPM containg nine LWIR photodiodes, baked at 65° C for over 1400 hours, showed no increase in noise for all but one of the photodiodes. The one showing minimal increase in noise. For the λ_c ~ 9 μm photodiodes the average value of $\alpha = 1.3 \times 10^{-4}$ in the dark and $\alpha_{PHOTO} \sim 2 \times 10^{-6}$ under illuminated conditions. The λ_c ~ 15 μm photodiodes have values of α in the low 10^{-5} range, with the highest performance, diffusion current limited photodiodes having

values of α in the mid 10^{-6} range. All the 850 μm diameter, $\lambda_c \sim 15$ μm photodiodes measured have excess low frequency noise, with the best performers having i_n(f = 100 Hz, V_d =-60 mV , Δf = 1 Hz) ~ 2 x 10^{-11} A/$Hz^{1/2}$.
In addition, other lessons learned were that a photodiode can exhibit "popcorn" noise from switching between two current states. However, this was observed once, the photodiode annealing out the damage from a warm-up and subsequent cooldown.

5.0 ACKNOWLEDGEMENTS

This work was performed on the CrIS program. The authors thank Capt. C. Muth (USAF and NPOESS IPO), Dr. D. Mooney (MIT/LL), Dr. M. Kelly (MIT/LL), Dr. F. Sabet-Peyman (Northrup-Grumman), Dr. A. Schwalb (NPOESS IPO), Dr. S. Kohn (Aerospace Corp.) and Dr. R. Schoolar (Aerospace Corp.) for their technical help. Thanks to our colleagues here at DRS Sensors & targeting Systems who have contributed to this effort in numerous ways.

6.0 REFERENCES

1. J. Bajaj, J.M. Arias, M. Zandian, D.D. Edwall, J.G. Pasko, L.O. Bubulac, and L.J. Kozlowski, J. Electron. Mater. 25, 1394 (1996).
2. A.I. D'Souza, L.C. Dawson, C. Staller, P.S. Wijewarnasuriya, R.E. DeWames, W.V. McLevige, J.M. Arias, D. Edwall, G. Hildebrandt, *J. Electron. Mater.* **29**, 630 (2000).
3. A.I. D'Souza, L.C. Dawson, E.J. Anderson, A.D. Markum, W.E. Tennant, L.O. Bubulac, M. Zandian, J.G. Pasko, W.V. McLevige, D.D. Edwall, J. Electron. Mater. 26, 656 (1997).
4. H. Holloway, *J. Appl. Phys.* , **49**, 4264 (1978)
5. P.S. Wijewarnasuriya, M. Zandian, D.B. Young, J. Waldrop, D.D. Edwall, W.V. McLevige, J. Arias, A.I. D'Souza, *J. Electron. Mater.* **28**, 649 (1999).
6. A.I. D'Souza, P.S. Wijewarnasuriya, R.E. DeWames, G. Hildebrandt, J. Bajaj, D.D. Edwall, J.G. Pasko, J.M. Arias, J. of Electronic Materials, 28, 611 (1999).
7. A.I. D'Souza, L.C. Dawson, S. Marsh, R. Willis, P.S. Wijewarnasuriya, R.E. DeWames, J.M. Arias, J. Bajaj, G. Hildebrandt, F. Moore, "Proceedings SPIE Aerosense ", Orlando, April 2001, Vol. 4369, pg. 157(2001).
8. A.I. D'Souza, M.G. Stapelbroek, S.A. Masterjohn, P.S. Wijewaarnasuriya, R.E. DeWames, G.M. Williams, Proceedings of SPIE Vol. 4721, Pg. 227.
9. A.I. D'Souza, M.G. Stapelbroek, P.N. Dolan, P.S. Wijewaarnasuriya, R.E. DeWames, D.S. Smith, J.C. Ehlert, *J. Electron. Mater.* **32**, 633 (2003).

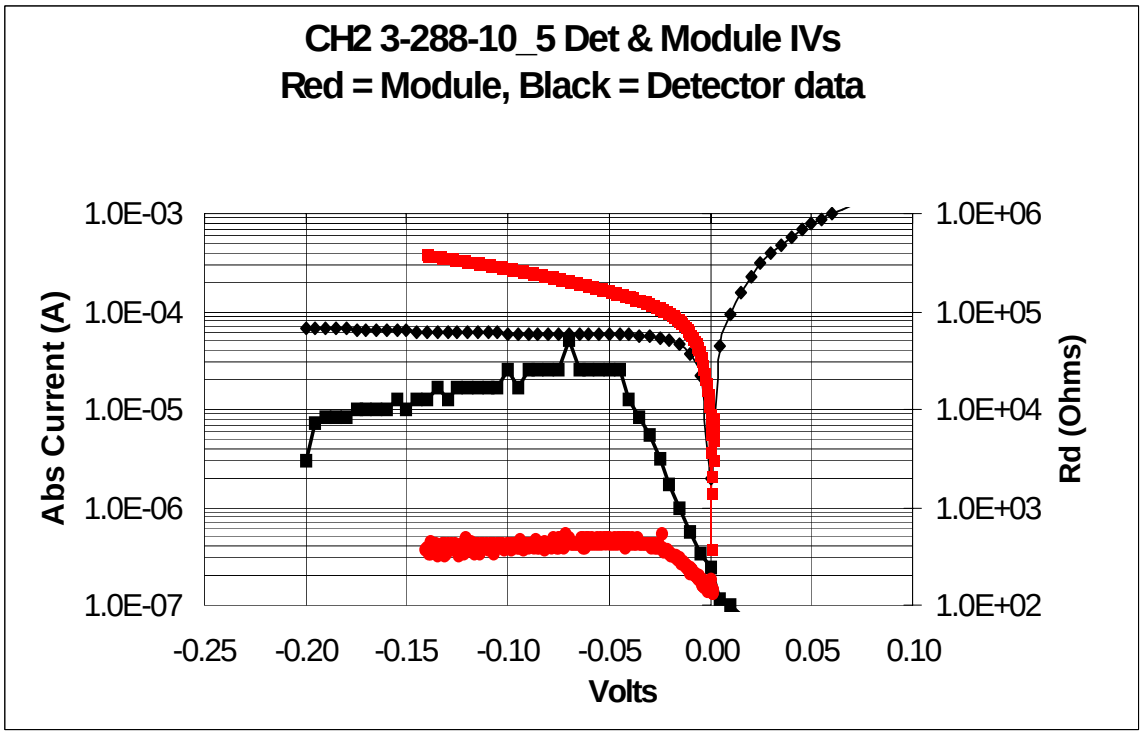

Figure 1. Dark I_d-V_d and R_d-V_d at 81 K for a LWIR λ_c(81K) ~ 15 μm photodiode at the LCC and FPM level

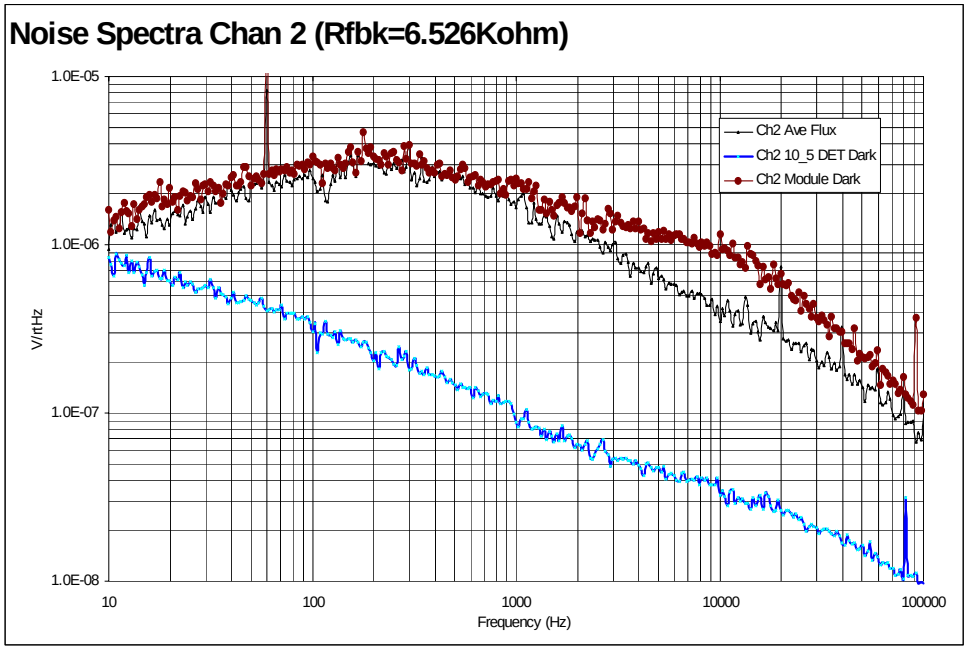

Figure 2. Noise versus frequency at 81 K at V_d = -60 mV for the LWIR λ_c(81 K) ~ 15 μm photodiode shown in figure 2 at the LCC and FPM level

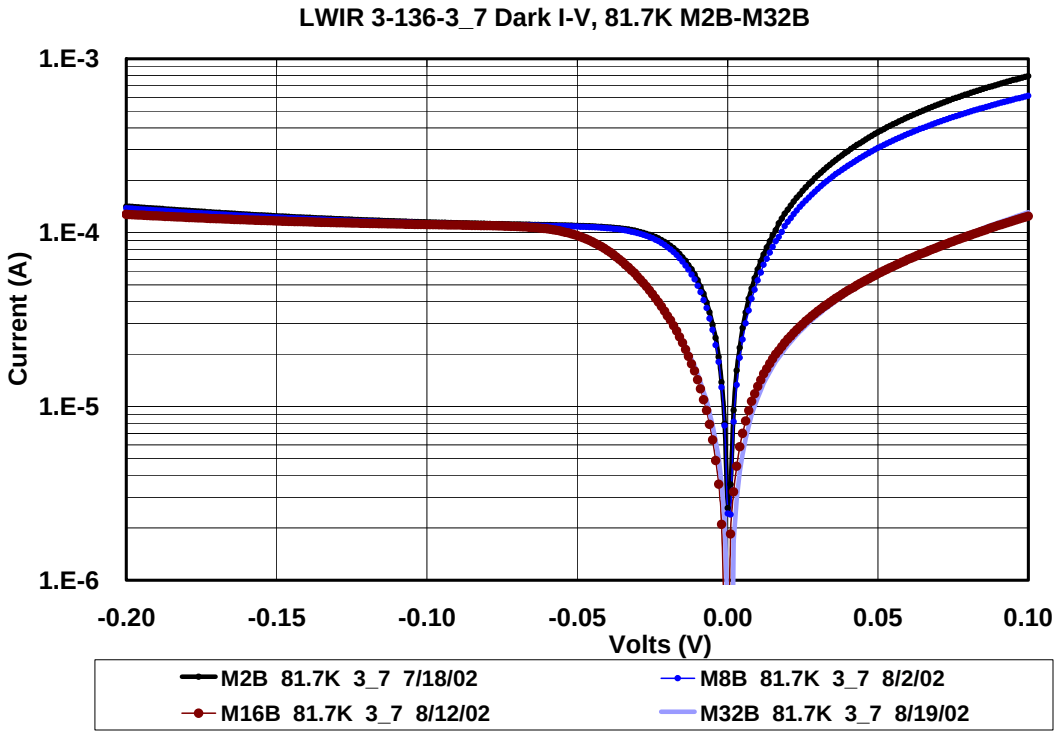

Figure 3. Dark I_d-V_d at 81.7 K for a LWIR λ_c(81 K) ~ 15 μm photodiode as a function of cumulative bake time at 90 C.

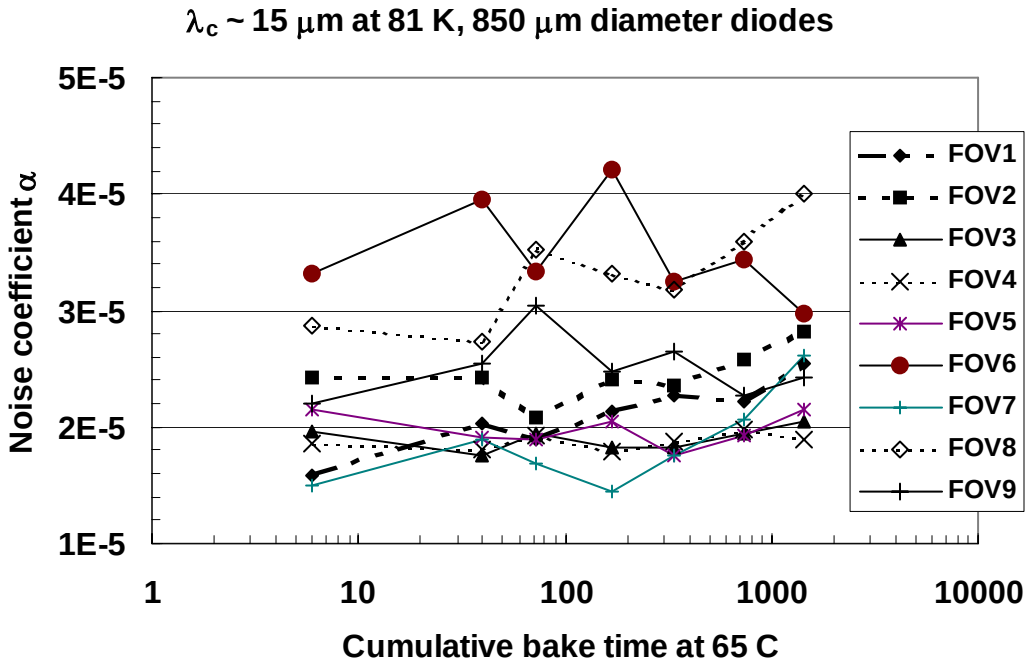

Figure 4. The ratio α, defined as the noise current in unit bandwidth i_n(f = 1 Hz, V_d , Δf = 1 Hz) to the dark current I_d(V_d), as a function of bake time at 65 C for nine λ_c ~ 14.5 μm photodiodes in a FPM

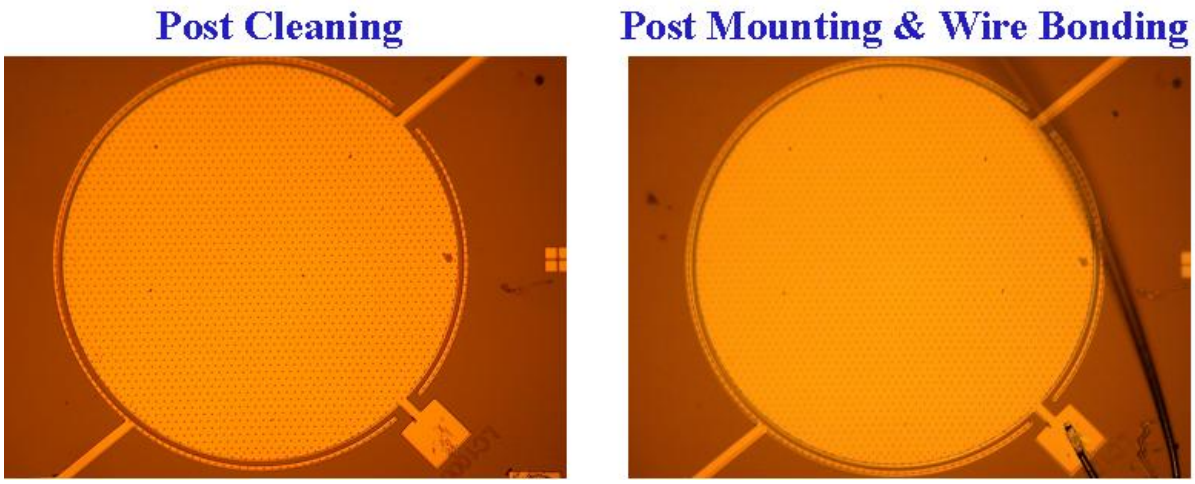

Figure 5a. Photographs of the top surface of a LWIR λ_c(81 K) ~ 15 μm photodiode following removal from the LCC and after mounting and wire bonding on a module. No visual changes.

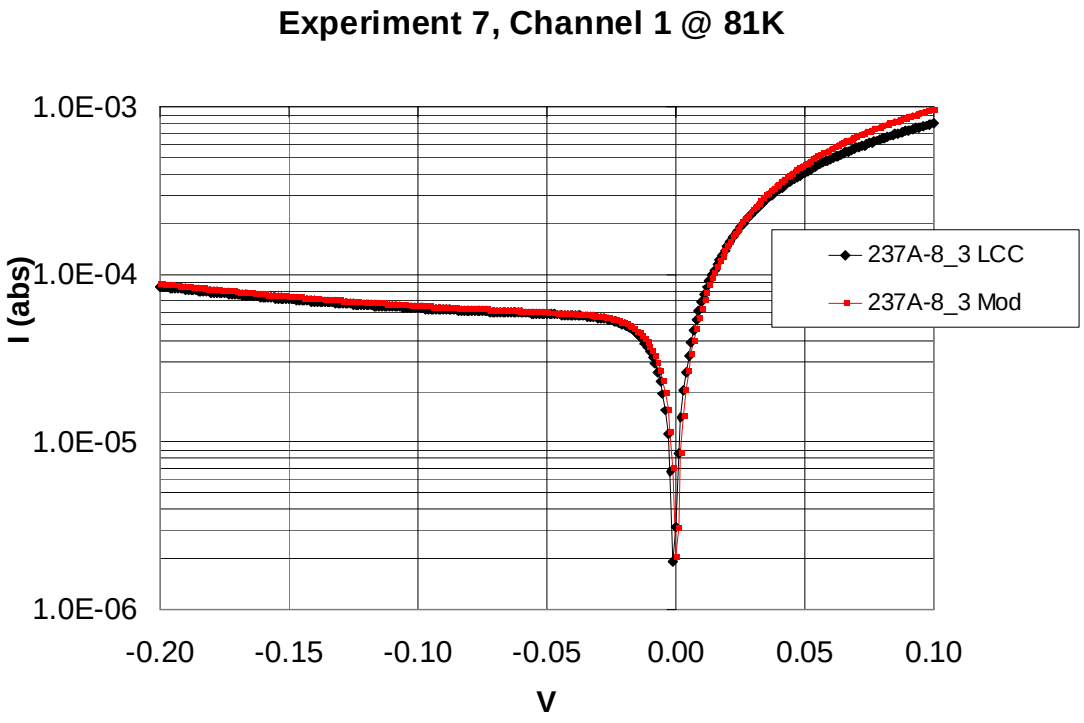

Figure 5b. Dark I_d-V_d at 81 K for the LWIR λ_c(81 K) ~ 15 μm photodiode shown in figure 5.

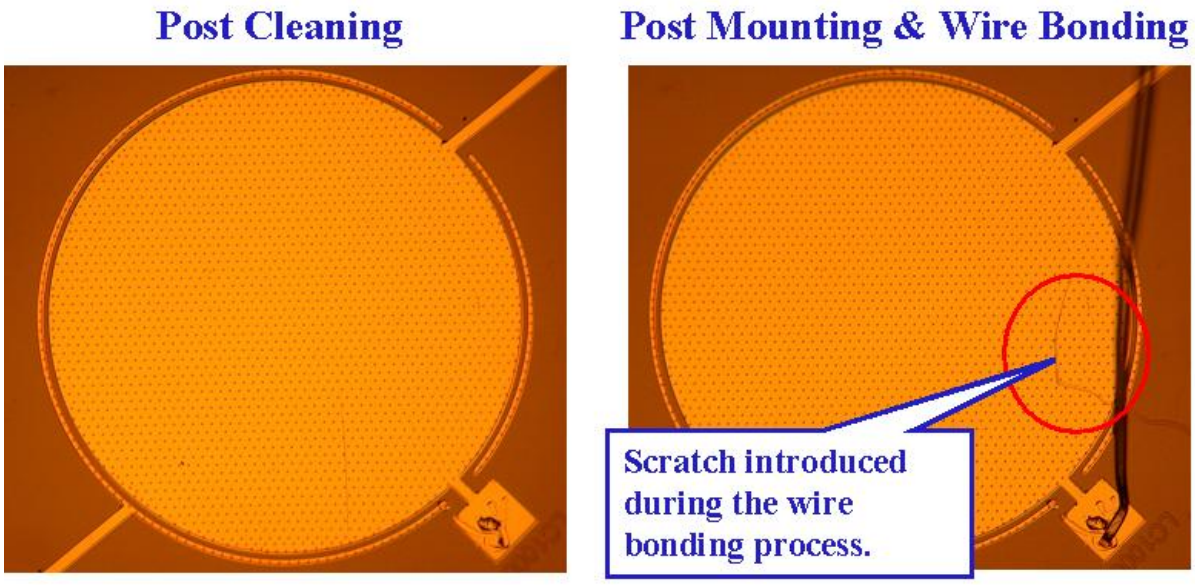

Figure 6a. Photographs of the top surface of a LWIR λ_c(81 K) ~ 15 μm photodiode following removal from the LCC and after mounting and wire bonding on a module. Scratch rising from wire bonding indicated.

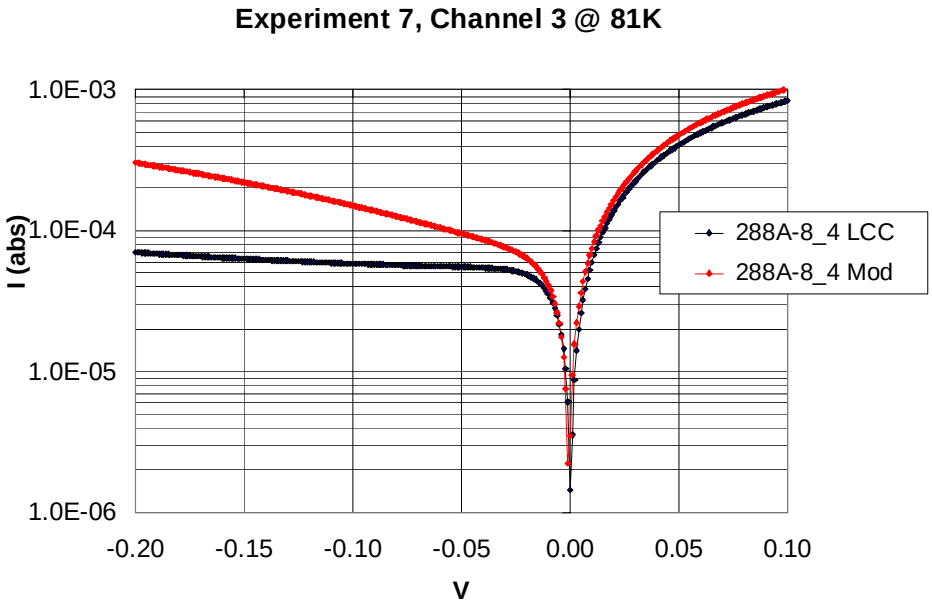

Figure 6b. Dark I_d-V_d at 81 K for the LWIR λ_c(81 K) ~ 15 μm photodiode shown in figure 6.

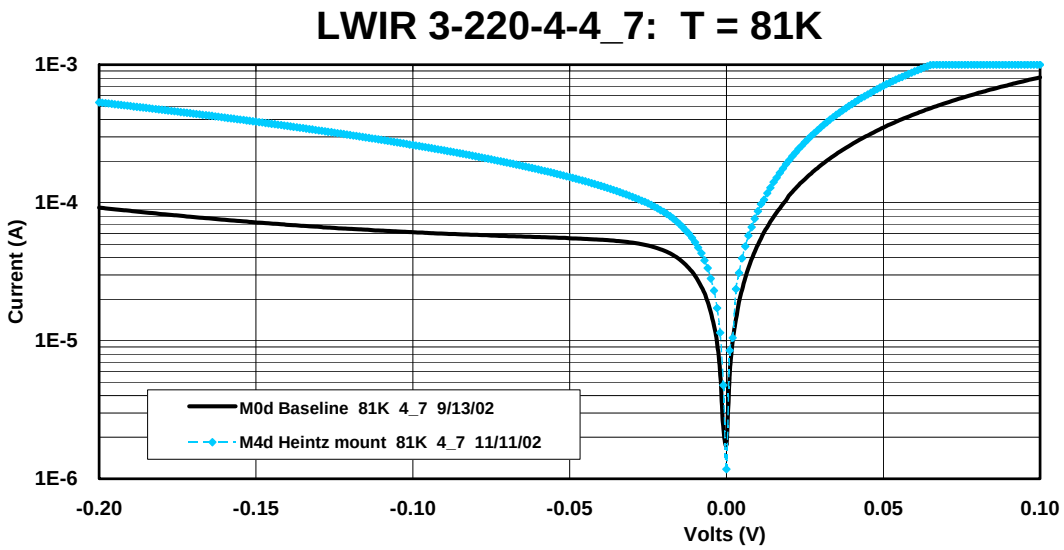

Figure 7. LWIR [λ_c(81 K) ~ 15 μm] I_d-V_d at 81 K before and after damage to the *p*-side metal caused during precision mounting on the Focal Plane Module

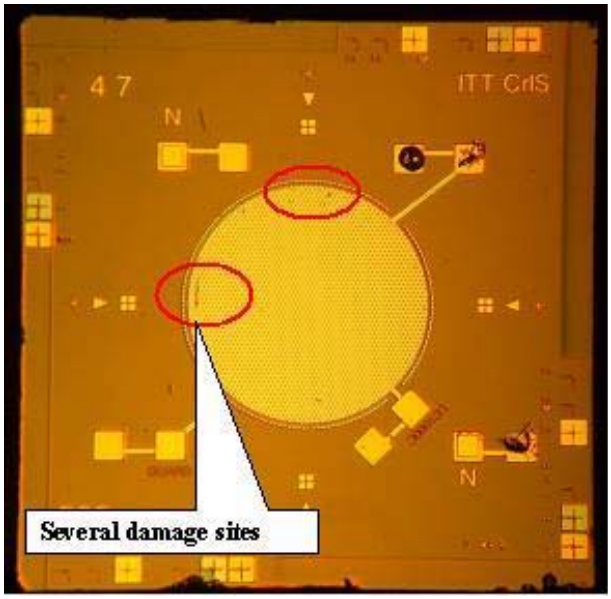

Figure 8. Photograph indicating *p*-side metal damage following precision mounting

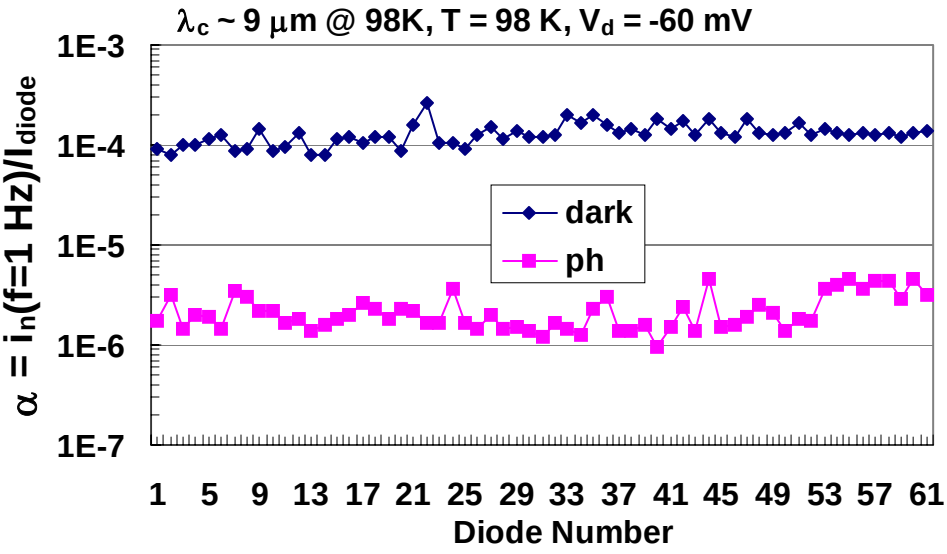

Figure 9. Noise coefficient α for λ_c(98 K) ~ 9 μm cutoff photodiodes under dark and illuminated conditions

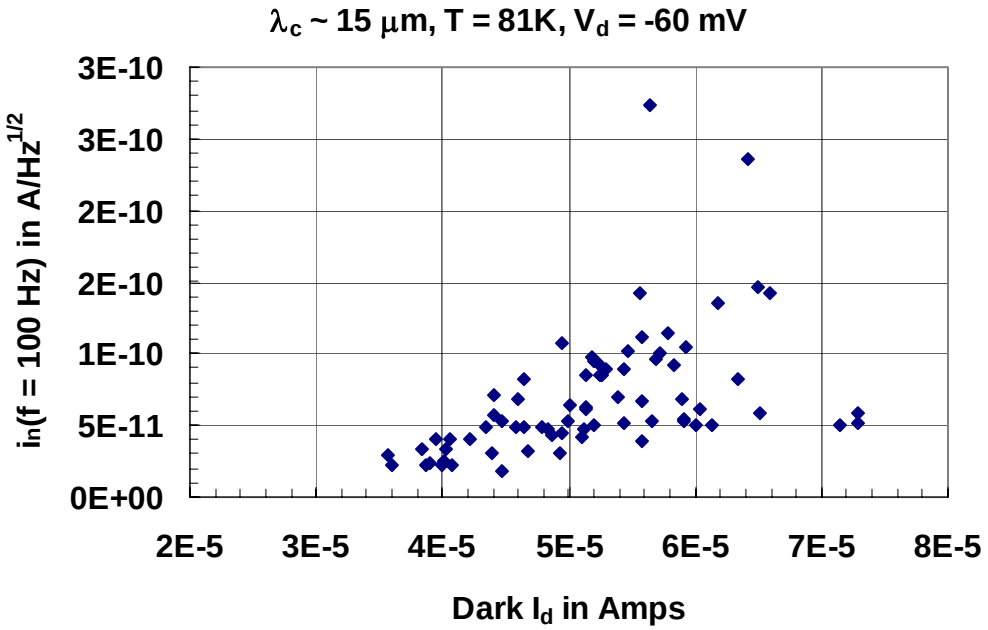

Figure 10a. Noise at 100 Hz versus photodiode current for λ_c(81 K) ~ 15 μm photodiodes under low background conditions

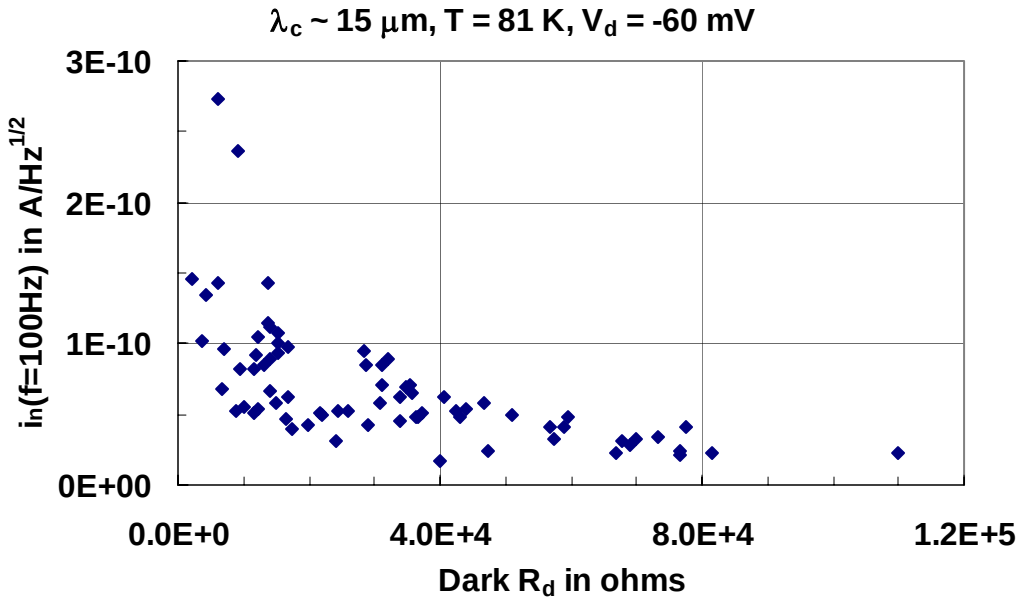

Figure 10b. Noise at 100 Hz versus diode dynamic impedance for λ_c(81 K) ~ 15 μm photodiodes under low background conditions

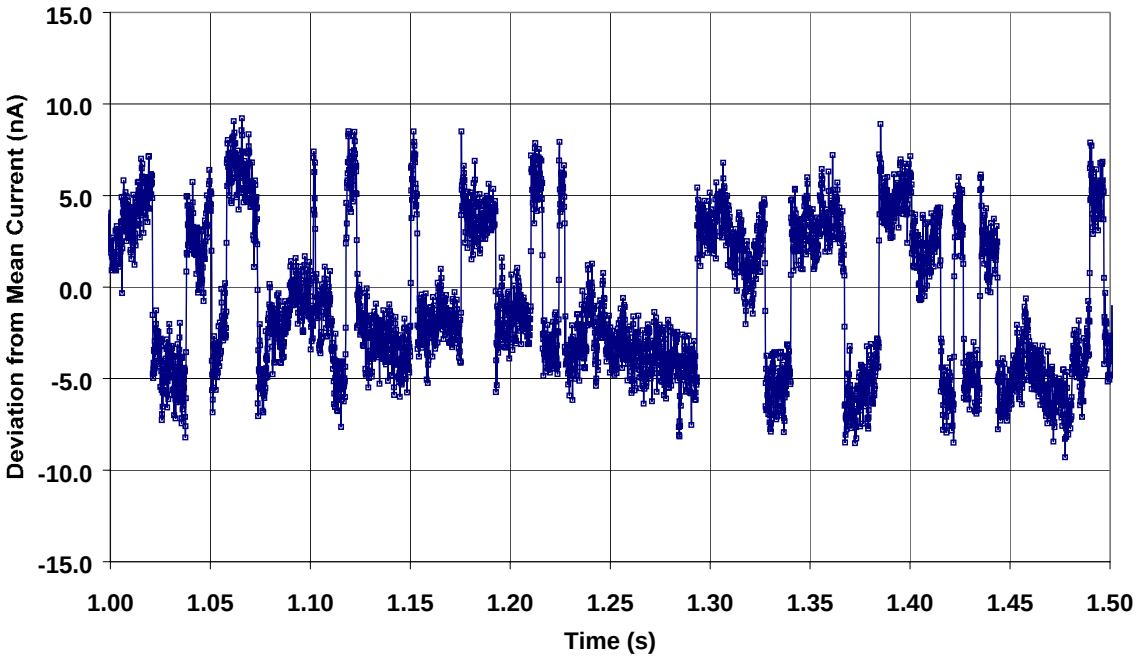

Figure 11. Time Series captured by Dynamic Signal Analyzer

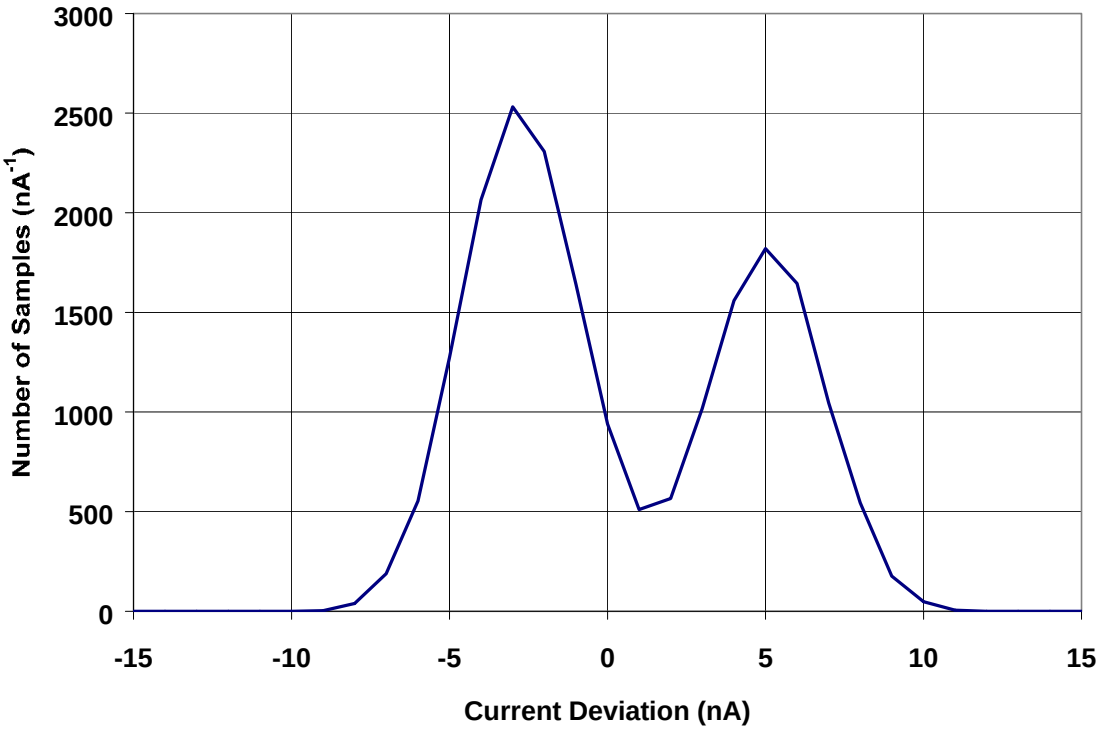

Figure 12. Histogram of Current Data

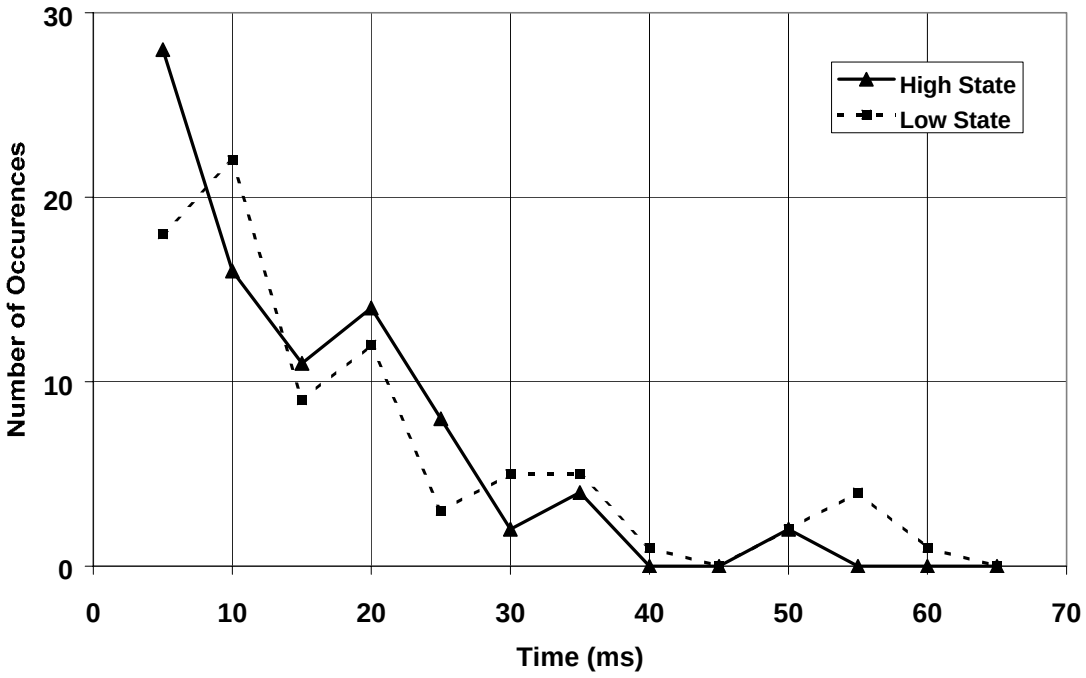

Figure 13. Number of occurrences versus time in each state